ECLÉTICA QUÍMICA

Eclet. Quim. 50 | e-1555, 2025

Original Article

https://doi.org/10.26850/1678-4618.eq.v50.2025.e1555

Immunoinformatics designing of peptide-based vaccine for malaria infection

James Akinwumi **Ogunniran**[1,2+], Elijah Kolawole **Oladipo**[1,3], Kemiki Olalekan **Ademola**[4], Anthony Godswill **Imolele**[5], Olaoluwa Kehinde **Alao**[6], Kehinde Oluyemi **Ajayi**[6], Michael Asebake **Ockiya**[7], Oluseyi Rotimi **Taiwo**[8], Caleb Enejoh **Omede**[9], Samuel Nzube **Nwosu**[10], Adeola Christianah **Ogunwole**[11]

Abstract

Malaria, a life-threatening disease prevalent in tropical regions, primarily affects infants, children under five, pregnant women, travelers, and individuals with HIV/AIDS. This study utilized an immunoinformatics approach to design a peptide-based malaria vaccine targeting antigenic proteins, including Apical Membrane Antigen 1, Knob-Associated Histidine-Rich Protein, Merozoite Surface Protein 1, and Sporozoite Surface Protein 2. Antigenic protein sequences were screened for antigenicity, allergenicity, toxicity, and immune responses involving CTLs, B-cells, and HTLs. Selected epitopes were linked with appropriate linkers and an adjuvant to enhance immunogenicity, forming a vaccine construct. The construction, comprising 1473 amino acids, exhibited a molecular weight of 15.21 kDa, a theoretical pI of 8.94, an aliphatic index of 60.01, and an instability index of 31.66, indicating stability. It was hydrophilic (GRAVY: –0.385) with favorable half-lives in mammalian, yeast, and *E. coli* systems. Docking studies showed strong binding affinity to human TLR2 and TLR4. In silico cloning indicated a CAI value of 0.92 and a GC content of 59.31%. Further studies are needed to validate its efficacy and safety.

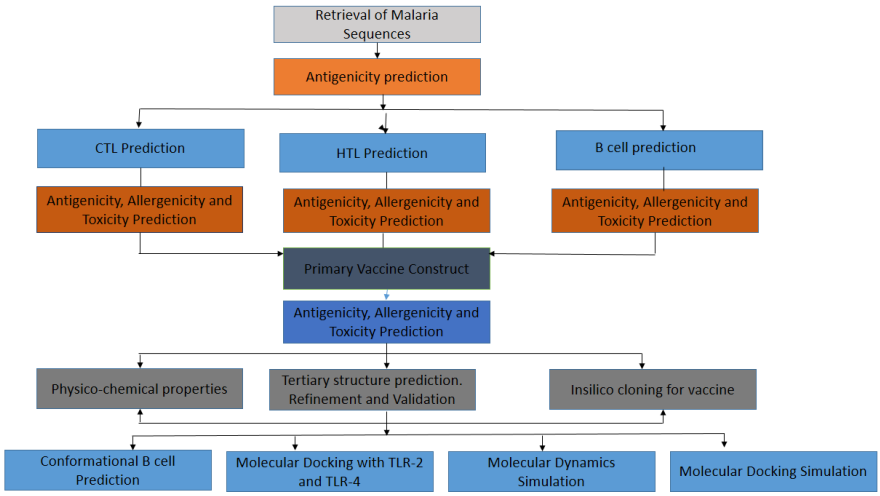

Article History

Received April 22, 2024
Accepted December 05, 2024
Published May 25, 2025

Keywords

1. malaria vaccine;
2.immunoinformatics;
3.antigenic proteins;
4.epitope prediction;
5.molecular docking.

Section Editors

Marcos Carlos de Mattos

Highlights

- Malaria is caused by Plasmodium parasites, transmitted by Anopheles mosquitoes.
- It is lethal and affects vulnerable populations like children and pregnant women.
- Current vaccines, like RTS, S, offer limited protection.
- New vaccine approaches focus on multi-epitope designs to enhance immune responses.
- Vaccines incorporate CTL, HTL, B-cell epitopes, enhancing protection against malaria.

[1]Helix Biogen Institute, Division of Vaccine Design and Development, Ogbomosho, Nigeria. [2]Ladoke Akintola University of Technology, Department of Medical Microbiology and Parasitology, Ogbomosho, Nigeria. [3]Adeleke University, Laboratory of Molecular Biology, Immunology and Bioinformatics, Ede, Nigeria. [4]Babcock University Teaching Hospital, Molecular and Tissue culture Laboratory, Ilishan-Remo, Nigeria. [5]Ambrose Alli University, Department of Biochemistry, Ekpoma, Nigeria. [6]Precious Cornerstone University, Department of Natural Science, Ibadan, Nigeria. [7]Department of Animal Science, Niger Delta University, Wilberforce Island, Bayelsa. [8]Clemson University, Department of Microbiology, Clemson, United States. [9]University of Colombo, Institute of Biochemistry, Molecular Biology and Biotechnology, Colombo, Sri Lanka. [10]University of Ilorin, Department of Forest Resources Management, Ilorin, Nigeria. [11]Ladoke Akintola University of Technology, Department of Community/Public Health Nursing, Ogbomosho, Nigeria. **+Corresponding author:** James Akinwumi Ogunniran, **Phone:** +2348031315189, **Email address:** ogunniranjames2017@gmail.com

1. Introduction

Malaria is regarded as one of the most lethal and incapacitating infectious diseases, marked by intermittent bouts of high fever. Its cerebral form is particularly concerning, as it can lead to severe neurological complications such as brain damage and coma (Pandey *et al.*, 2017). The global incidence of malaria cases has been alarmingly high, reaching 247 million in 2021, 245 million in 2020, and 232 million in 2019 (WHO, 2022). Specific populations are particularly vulnerable to malaria infection, including children under the age of 5, HIV-positive individuals, pregnant women (Schumacher *et al.*, 2012), and travelers (Chaves *et al.*, 2017). The protozoan parasite Plasmodium is the causative agent of malaria, transmitted to humans through the bite of previously infected female Anopheles mosquitoes (Biamonte *et al.*, 2013). Among humans, malaria infection is caused by several species of the Plasmodium genus, including *P. falciparum*, *P. ovale, P. malariae,* and *P. vivax* (Amir *et al.*, 2022). A newly identified species, *P. knowlesi*, has been recognized in Southeast Asian countries, particularly Malaysia, as the sixth species causing malaria infection (Singh *et al.*, 2004). *P. vivax* is commonly associated with the sub-Saharan region of Africa and contributes significantly to morbidity, while *P. falciparum*, the most severe type of parasite, is prevalent in Africa and is responsible for most malaria-related deaths (Amir *et al.*, 2022). The malaria parasite's life cycle consists of four phases: the liver stage, blood stage, human transmission stage, and mosquito stage. Each stage must be considered for effective therapy to achieve complete eradication of the disease (Crompton *et al.*, 2010).

After being released from the mosquito bite, sporozoites migrate into the bloodstream from the bite site and invade hepatocytes in the liver (Lindner *et al.*, 2012). In the liver stage, the parasites undergo proliferation for approximately seven days (a week) before releasing exo-erythrocytic merozoites into the bloodstream to initiate the blood stage of infection (Sinnis *et al.*, 2008). Recurrent cycles of replication during the blood stage of infection lead to an exponential increase in the number of malaria parasites and the manifestation of all clinical symptoms associated with malaria (Kristian *et al.*, 2016). Before the initiation of the symptomatic stage of the disease, the parasite can be eliminated by targeting the asymptomatic sporozoite and liver stage parasites when parasite populations are low (Kristian *et al.,* 2016). Additionally, peptides or antibodies that block the AMA1-RON2 connection reduced the *Plasmodium merozoites'* capacity to colonize the host cells (Srinivasan *et al.*, 2011). The protein known as AHRP, or knob-associated histidine-rich protein (KAHRP) is usually produced when *Plasmodium falciparum* initiates infection in the erythrocytes (Maier *et al.,* 2009). A glycosylphosphatidylinositol-anchored protein known as merozoite surface protein 1 (MSP1), which constitutes the larger part of the merozoite surface protein, has been identified by researchers as a potential vaccination candidate (Holder *et al.,* 2009). This 190–200 kDa protein is attached to the surface of the merozoite by a glycosylphosphatidylinositol at its C-terminus (Holder *et al.*, 2009). Although it is yet unknown how the MSP1 merozoite surface complex affects erythrocyte invasion, recombinant fragments and variants of MSP1 produced from parasites have been associated with the binding of erythrocyte receptors (Kadekoppala *et al.*, 2008).

A key challenge in developing an effective malaria vaccine is the parasite's multistage life cycle complexity. This complexity indeed imposed a significant obstacle to vaccine development, as targeting each life cycle stage requires a deep understanding of the parasite's biology and host immune responses at various stages (Amlabu *et al.*, 2018). The initial malaria vaccine, RTS, S (also known as Mosquirix), which is based on recombinant proteins, has demonstrated only modest effectiveness in protecting young children against the disease. (Amir *et al.*, 2022). Despite considerable endeavors, this vaccination approach has drawbacks, as it only averts 39% of malaria infections and 30% of severe malaria cases (Amir *et al.*, 2022). After several months, its effectiveness diminishes, requiring four doses for optimal protection (Laurens *et al.*, 2020).

This research recommends creating a peptide-based vaccine containing immune-stimulating epitopes capable of eliciting both humoral and cell-mediated immune responses to prevent malaria infection.

2. Experimental

2.1. Systematic workflow

This study adhered to a systematic workflow, as depicted in Fig. 1. The diagram outlines each step involved in formulating this multi-epitope vaccine.

2.2. Protein sequence retrieval

The protein sequences of Plasmodium falciparum were retrieved from the National Center for Biotechnology Information (NCBI) (Oladipo *et al.*, 2024a) and the Universal Protein Resource (UNIPROT) Server. Apical membrane antigen 1(A0A0X8II02), Apical membrane antigen 1(A0A193PBV5), Knob associated histidine-rich protein (A0A0L7KKR3), Knob associated histidine-rich protein (W7FDY3), Merozoite surface protein 1(Q25971), Sporozoite surface protein 2(A0A0L0CV98), Sporozoite surface protein 2(A0A0L7KJ49).

2.3. Prediction of protein sequence antigenicity

The antigenicity of the *Plasmodium falciparum* protein was predicted using ANTIGENpro (Magnan *et al.*, 2010) and VaxiJen (Pandey *et al.*, 2016). The threshold of ≥0.8 (ANTIGENpro) (Magnan *et al.,* 2010), and ≥ 0.5 VaxiJen (Doytchinova *et al.,* 2007) were considered for the selection of the protein sequence.

2.4. Cytotoxic T lymphocytes (CTL) epitopes prediction

NetCTL 1.2 tool was utilized in the prediction of CTL epitopes of the proteins (Oladipo *et al.*, 2020). The tool was set at a threshold value of 0.75, while the weights on C-terminal cleavage and TAP transport efficiency were set at 0.15 and 0.05, respectively (Zhao *et al.,* 2017).

2.5. Helper T-Cell (HTL) epitope prediction

The HTL Epitopes of the protein sequence were predicted using the Immune Epitope Database (IEDB) (Oladipo *et al.*, 2022). Three mouse alleles, which are H2-IAb, H2-IEd and H2-IAd, were selected for the Major Histocompatibility Class II (MHC II). MHC-II affinity and percentile rank of ≤ 0.2 were used as criteria for selecting the HTL epitopes (Zhang *et al.,* 2008). The best six epitopes were chosen for each allele.

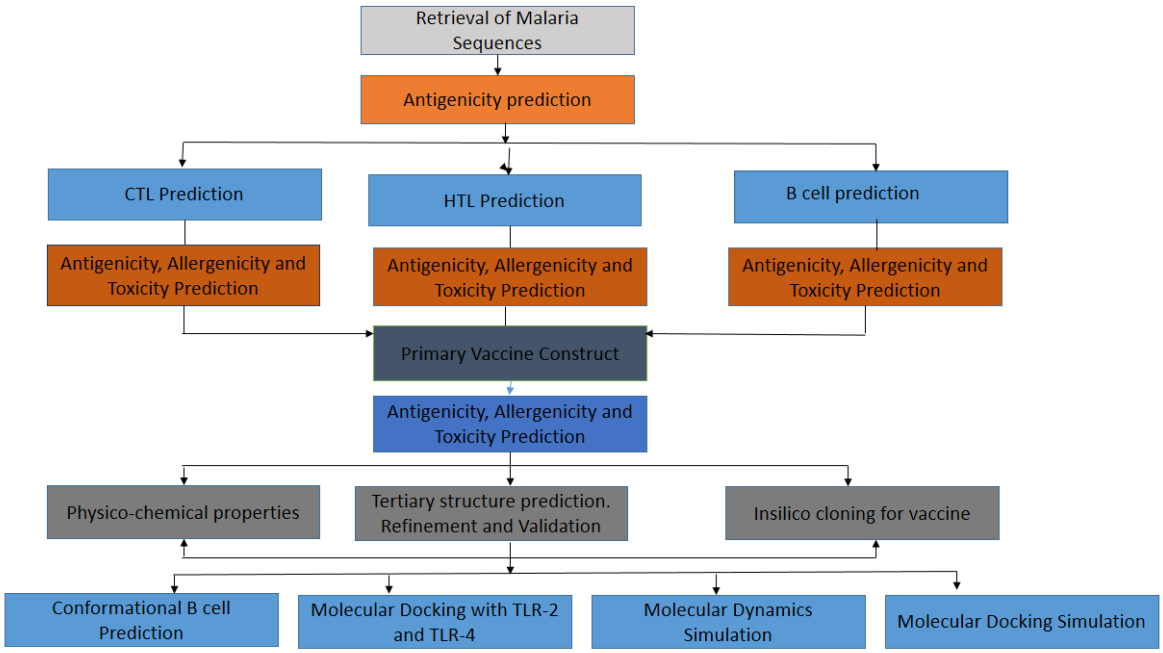

Figure 1. Study workflow for malaria vaccine construct design.
Source: Elaborated by the authors.

2.6. B-Cell epitopes prediction

B-cells are an important component of the immune system for long-term protection against pathogens and antigens (Oladipo *et al.*, 2022). The linear B-cell Epitopes of *Plasmodium falciparum* protein were predicted using ABCPred server (Saha and Raghava, 2006). Eight epitopes with a score > 0.9 were selected and subjected to further analysis.

2.7. Construction of multi-epitope vaccine sequence

A multi-epitope vaccine was developed by combining cytotoxic T lymphocyte (CTL), helper T lymphocyte (HTL), and B-cell epitopes, joined with an adjuvant using appropriate linkers. The adjuvant APPHALS was incorporated to enhance the vaccine's immunogenicity. AAY linkers were utilized to connect the CTL epitopes, whereas GPGPG linkers were employed to connect the HTL and B-cell epitopes (Kalita *et al.*, 2019).

2.8. Antigenicity, allergenicity and toxicity prediction of the vaccine construct

The antigenicity, allergenicity, and toxicity of the vaccine construct were assessed using the VaxiJen (Doytchinova *et al.*, 2007), Allertop (Dimitrov *et al.*, 2014), and Toxinpred2 (Sharma *et al.*, 2022) servers, respectively. Antigenicity testing confirmed the vaccine's ability to stimulate antibody production. Allergenicity assessment was conducted to verify the absence of allergic reactions triggered by the vaccine. Toxicity testing was performed to ensure the vaccine's safety by confirming the absence of adverse effects on humans.

2.9. Physiochemical properties and domain identification

The physicochemical properties of the vaccine construct, including molecular weight, theoretical protrusion index (PI), hydropathicity (GRAVY), aliphatic index, instability index, extinction coefficients, atomic composition, charged residues, and in vitro and in vivo half-life, were analyzed using protparam (Garg *et al.*, 2016).

2.10. Prediction of secondary structure

The self-optimized prediction method (SOPMA) was utilized to predict the secondary structure of the vaccine construct. SOPMA analyzes the amino acid composition and predicts the relationships within the construct's secondary structure (Lee *et al.*, 2013).

2.11. Prediction of tertiary structure of the vaccine

The tertiary structure of the multi-epitope vaccine construct was predicted using I-TASSER (Zhou *et al.*, 2022). The I-TASSER tertiary structure prediction server is designed to generate protein tertiary structures and employs a quantitative scoring system to produce models. Additionally, the server predicts estimated TM-score, confidence score, standard deviation, and root mean square deviation (RMSD) values for the generated models.

2.12. Prediction of 3D configuration and discontinuous B-cell epitopes

The tertiary composition of the vaccine construct was utilized to predict the 3D conformational structure of B-cell epitopes using Ellipro. Subsequently, Ellipro was employed to determine the conformational 3D structure of the predicted linear B-cell epitopes. The Ellipro results include the number of residues in each epitope, with higher residue numbers indicating greater solvent availability. The Jmol viewer was utilized for visualizing the predicted antibody epitopes (Ponomarenko *et al.*, 2008).

2.13. Refinement of the tertiary structure

To enhance the quality of the local structure in the multi-epitope vaccine construct, the Galaxy Refine web tool, based on

the CASP 10 version, was employed (Heo *et al.,* 2013). Galaxy Refine is a validated algorithm known for refining protein structures and improving the quality of local structural elements (Oladipo *et al*., 2023a).

2.14. Validation of tertiary structure

The ProSA-web server was utilized to validate both the projected and refined 3D configuration of proteins, an essential step in sequence modeling. Additionally, a Ramachandran plot was obtained by submitting the PDB file of the vaccine structure to the PROCHECK server. This process serves to validate the vaccine and authenticate its potential functionality (Laskowski *et al.*, 2006).

2.15. Molecular docking of the vaccine with toll-like receptors (TLRs)

Stimulating an immune response is the primary objective in vaccine design. Therefore, it is crucial to evaluate the interactions between an antigen and Toll-like receptors (TLRs). The HDock server was employed to predict the binding sites between TLR-2 (PDB ID: 3a7c) and TLR-4 (PDB ID: 4g8a) in their most stable complex forms. Docking analysis facilitated the examination of binding affinity between the complexes, specifically the vaccine and TLRs (Yan *et al.*, 2020).

2.16. Molecular dynamics simulation of the receptor-ligand complex

The iMOD server was utilized to conduct dynamics simulations, which focused on studying the physical basis, structure, and function of biological molecules to determine the stability of the complex. Results obtained from this approach, such as deformability, eigenvalues, and covariance, provide insights into the stability of the complex (López-Blanco *et al.*, 2014).

2.17. The *in silico* cloning and optimization of the vaccine protein

The vaccine construct underwent codon optimization using the JCAT Java tool. This tool translates protein sequences into the expression system of another biological host to adapt the codon usage for the new host. JCAT provides the GC content and codon adaptation index (CAI) values of the adapted codons. Additionally, the tool back-translates protein sequences into DNA sequences, which are then used for silicon cloning. In this study, JCAT was employed to adjust the final vaccine sequences to fit the *E. coli* K12 strain expression system. The construct of the final vaccine was input into JCAT for adaptation processing (Grote *et al.*, 2005). The DNA sequences obtained from back-translation were cloned into the *E. coli* K12 pET-28a (+) vector expression system at specific restriction enzyme sites, with the assistance of Snap Gene software (Li *et al.*, 2016).

3. Result and discussion

3.1. Antigenicity prediction of *Plasmodium falciparum* proteins

The NCBI and Uniprot servers were used to obtain the *Plasmodium falciparum* protein sequence for this work. A critical component of vaccinology was achieved when the chosen sequences underwent antigenic screening and were proven to be both antigenic. The antigenicity of the *Plasmodium falciparum* proteins retrieved was predicted, and the sequences passed the AntigenPRO server and VaxiJen server at a threshold of 0.5 and 0.8, respectively (Table 1). This shows that the sequence can elicit antibodies (Oladipo *et al.,* 2022). The sequences that passed were then subjected to further analysis.

Table 1. Selected proteins of *Plasodium falciparum* and their accession number.

S/N	PROTEIN	ACCESSION NO	VAXIJEN	ANTIGENIC PRO
1	Apical membrane antigen 1	A0A0X8II02	0.6195	0.940153
	Apical membrane antigen 1	A0A193PBV5	0.5807	0.936320
2	Knob associated histidine-rich protein	A0A0L7KKR3	0.7862	0.940365
	Knob associated histidine-rich protein	W7FDY3	0.7880	0.922167
3	Merozoite surface protein 1	Q25971	0.5735	0.810633
4	Sporozoite surface protein 2	A0A0L0CV98	0.6279	0.902585
	Sporozoite surface protein 2	A0A0L7KJ49	0.6223	0.905200

Source: Elaborated by the authors.

3.2. Prediction of novel cytotoxic T lymphocytes (CTL), helper T lymphocytes (HTL) and B-cells epitopes

Different servers were employed to project CTL, HTL, and B-cell epitopes using the selected Plasmodium falciparum protein sequences that successfully passed antigenicity screening. CTL epitopes were identified based on their high scores, which fell within the threshold of 0.75 (Table 2a). Helper T lymphocytes (HTL) epitopes were also predicted, and those with low percentile ranks were chosen for further analysis (Table 2b). B-Cell epitopes falling within the threshold of 0.90 were selected (Table 2c) and incorporated into the vaccine construction alongside the HTL and CTL epitopes. The prediction of CTL, HTL, and B-Cell epitopes was conducted because a multi-epitope vaccine necessitates the inclusion of CTL, HTL, and B-Cell epitopes (Chauhan *et al.*, 2019). This is significant because T-cells recognize surface antigens presented by MHC molecules. MHC class II molecules present surface antigens to T-helper cells, while B-cell epitopes aid in eliciting antibody and memory cell responses (Oladipo *et al.,* 2022). The results obtained from these analyses were employed in building the vaccine candidate using appropriate linkers.

Table 2a. Selected epitopes of CTL.

Protein	CTL epitopes	Score	CTL epitopes	Score	CTL epitopes	Score
Apical membrane antigen 1	TLDQMRHFY	32.272	AQENNGPRY	0.9554	LLSAFEFTY	17.715
	ATILMVYLY	22.792	QYEQHLTDY	0.8786	DAEVAGTQY	14.733
	VLATILMVY	15.535	MVSNSTCRF	0.8368	AKDKSFQNY	11.252
	DISFQNYTY	15.338	VKEEYKDEY	0.8326	TLNGMRDFY	10.820
	AKDISFQNY	11.520	NTETHKCEI	0.7820	MLDPEASFW	0.8858
	ISDDKDSLK	11.379	IIENSNTTF	0.7664	GQNYWEHPY	0.7521
	SASDQPKQY	10.603	YMGNPWTEY	17.963		
Knob associated with histidine-rich protein	LDEYQNQLY	11.135	YAFSEECPY	0.8247	YVPPHGAGY	10.598
Merozoite surface protein 1	HLEAKVLNY	28.435	YLKPLAGVY	12.527	QLENNVMTF	0.8661
	NLEKKKLSY	19.055	LLILMLILY	10.159	KRDKFLSSY	0.8435
	GIADLSTDY	15.242	QTEDNYASL	0.8765	ESIQTEDNY	0.7781
Sporozoite surface protein 2	LLACAGLAY	24.876	LNENAIHLY	14.074	LTDGIPDSI	0.9307

Table 2b. Selected epitopes of HTL.

Protein	Alleles	HTL epitope	Score	Alleles	HTL epitope	Score
Apical membrane antigen 1	H2-IAb	KDGGFAFPPTKPLMS	0.26	H2-IAd	IIIASSAAVAVLATI	0.73
	H2-IAb	DGGFAFPPTKPLMSP	0.37	H2-IAb	DLKDGGFAFPPTKPL	0.84
	H2-IAb	GGFAFPPTKPLMSPM	0.39	H2-IAd	DNMKIIIASSAAVAV	0.85
	H2-IAb	SMIKSAFLPTGAFKA	0.39	H2-IAb	GFAFPPTKPLMSPMT	0.87
	H2-IAb	MIKSAFLPTGAFKAD	0.40	H2-IAd	IIASSAAVAVLATIL	0.90
	H2-IAd	MKIIIASSAAVAVLA	0.46	H2-IAd	PTYDNMKIIIASSAA	0.91
	H2-IAb	IKSAFLPTGAFKADR	0.48	H2-IAd	YDNMKIIIASSAAVA	0.93
	H2-IAd	KIIIASSAAVAVLAT	0.58	H2-IAd	KPTYDKMKIIIASSA	0.37
	H2-IAb	LKDGGFAFPPTKPLM	0.58	H2-IAb	KSAFLPTGAFKADRY	0.60
	H2-IAb	KSAFLPTGAFKADRY	0.60			
Knob associated histidine-rich protein	H2-IEd	ENGPNIFALRKRFPL	0.65	H2-IEd	QENGPNIFALRKRFP	1.75
	H2-IEd	GPNIFALRKRFPLGM	0.79	H2-IAb	GSTTGATTGANAVQS	1.65
	H2-IEd	PNIFALRKRFPLGMN	0.84	H2-IAb	STTGATTGANAVQSK	1.70
	H2-IEd	SFKNKNTLRRKKAFP	1.65	H2-IAb	AGSTTGATTGANAVQ	1.95
	H2-IEd	FKNKNTLRRKKAFPV	1.75	H2-IAb	TTGATTGANAVQSKD	1.95
Merozoite surface protein 1	H2-IAb	KNKNYTGNSPSVNNT	1.00	H2-IAb	KNYTGNSPSVNNTDV	1.51
	H2-IAb	IKNKNYTGNSPSVNN	1.10	H2-IEd	KDPYKFLNKEKRDKF	1.90
	H2-IAb	VIKNKNYTGNSPSVN	1.10	H2-IEd	DPYKFLNKEKRDKFL	2.00
	H2-IAb	NKNYTGNSPSVNNTD	1.26			
Sporozoite surface protein 2	H2-IAb	LAYKFVVPGAATPYA	0.10	H2-IAb	DRYIPYSPLPPKVLD	0.23
	H2-IAb	AGLAYKFVVPGAATP	0.12	H2-IAb	RYIPYSPLPPKVLDN	0.30
	H2-IAd	KNKEKALIIIKSLLS	1.90	H2-IAb	YKFVVPGAATPFAGE	0.46
	H2-IAd	NKEKALIIIKSLLST	2.00	H2-IAb	KFVVPGAATPFAGEP	1.95
	H2-IAb	LAYKFVVPGAATPFA	0.10			

Table 2c. Selected epitopes of B-cell.

Protein	B-cell epitope	Position	Score
Apical membrane antigen 1	RFFVCKCVERRAEVTS	355	0.92
	MKIIIASSAAVAVLAT	397	0.90
	AFKADRYKSHGKGYNW	236	0.90
	MDEPQHYGKSNSRNDE	579	0.93
	ADIPEHKPTYDKMKII	533	0.91
Knob-associated histidine-rich protein	DNKGSEGYGYEAPYNP	290	0.90
Merozoite surface protein 1	SESGSDTLEQSQPKKP	100	0.90
Sporozoite surface protein 2	DRYIPYSPLPPKVLDN	410	0.94
	ERKQSDPQSQDNNGNR	426	0.92
	PEDSEKEVPSDVPKNP	365	0.91
	HGRNNENRSYNRKYND	454	0.90
	AGLAYKFVVPGAATPF	511	0.90

Source: Elaborated by the authors.

3.3. Construction of novel multiple epitope subunit vaccine

A multi-epitope vaccine was assembled using the predicted CTL, HTL, and B-cell binding epitopes. Linkers were utilized to connect these epitopes (Oladipo *et al.*, 2022), and an adjuvant was linked to the construction to enhance its potency and elicit a robust immune response (Oladipo *et al.*, 2022). Specifically, AAY linkers were employed to connect CTL epitopes, GPGPG linkers were used to link HTL and B-cell epitopes, and EAAAK linkers were utilized to attach the adjuvant to the vaccine construct (Ito *et al.*, 2017) as shown in **Fig. 2**.

Figure 2. The schematic representation of the malaria vaccine construct.
Source: Elaborated by the authors.

3.4. Physicochemical properties of the vaccine construct

The physicochemical properties of the vaccine construct predicted by Protparam indicate that the vaccine has a molecular weight of 15.21 kDa, falling within the range for an accepted vaccine candidate (Garg *et al.*, 2016). Our findings suggest that the vaccine construct is antigenic, non-toxic, and non-allergenic, indicating its safety. The theoretical pI value of 8.94 suggests a structurally favorable vaccine. The aliphatic index score of 60.01 indicates the presence of aliphatic side chains in the vaccine. In contrast, the instability index score of 31.66 predicts the vaccine to be stable (Oladipo *et al.*, 2023b). The GRAVY result of -0.385 indicates the hydrophobicity of immunization (Oladipo *et al.*, 2024b). Furthermore, the predicted half-life is 4.4 hours in mammalian reticulocytes in vitro, >20 hours in yeast, and 10 hours in *E. coli* in vivo.

3.5. Projection of secondary structure

SOPMA was employed to predict the secondary structure of the constructed vaccine. The server provided additional information on the vaccine construct, revealing an alpha helix content of 25.87%, an extended strand content of 15.55%, a random coil content of 54.04%, and a beta turn structure content of 4.55% (**Fig. 3** and **Table 3**). The high percentage of the random coil suggests a concentrated presence of epitopes at that point (Tahmoorespur *et al.*, 2017). The prediction of the secondary structure of our vaccine indicates stability, good flexibility, and a globular conformation, which aligns with the findings of Oluwagbemi *et al.* (2022).

Table 3. Parameter of the secondary structure prediction.

Parameters	No of Residues	Percentage
Alpha helix	381	25.87%
3_{10} helix	0	0
pi helix	0	0
Beta bridge	0	0
Extended strand	229	15.55%
Beta turn	0	0
Bend region	0	0
Random coil	796	54.04%
Ambiguous states	0	0
Other state	0	0

Source: Elaborated by the authors.

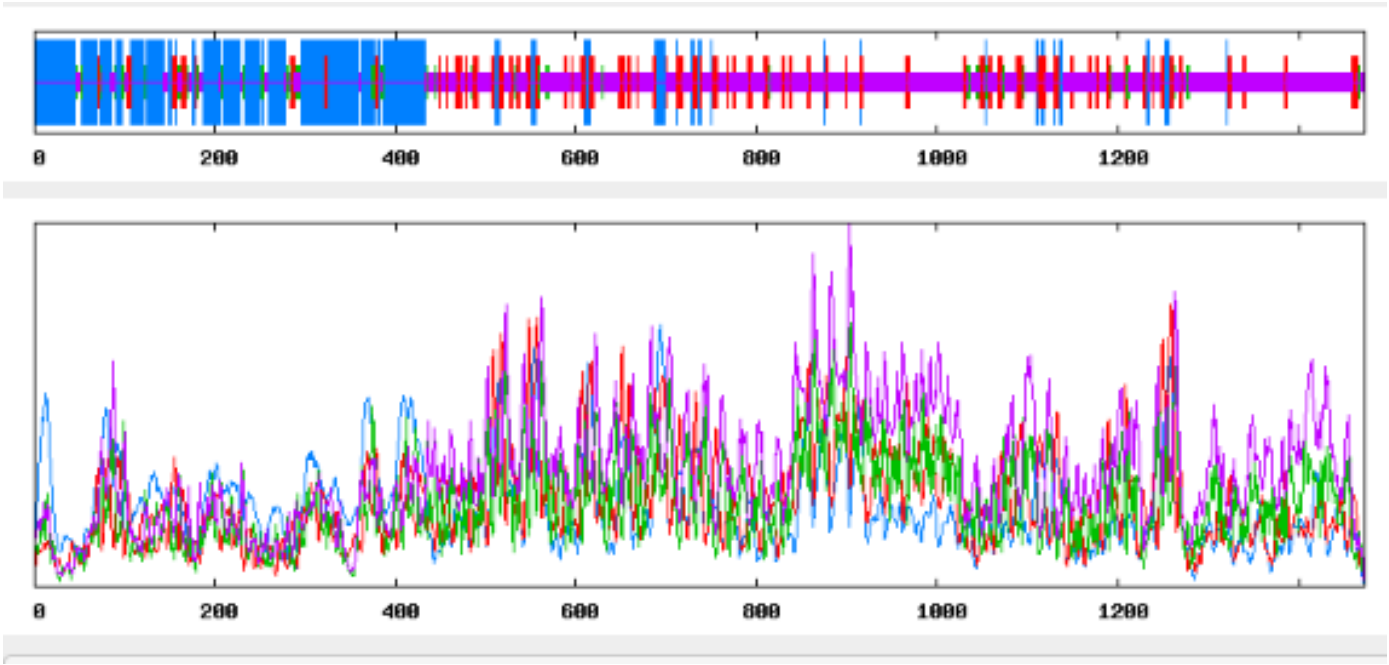

Figure 3. Prediction of the secondary structure of the constructed vaccine.
Source: Elaborated by the authors.

3.6. Prediction of the tertiary structure of the constructed vaccine

The I-TASSER server was employed to predict the 3D configuration of the multi-epitope vaccine construct. Five models were expected, but model 1 was chosen based on the confidence score of 0.19, the estimated TM-score of 0.74 ± 0.11, and the Root Mean Square Deviation (RMSD) of 9.4 ± 4.6 Å (Fig. 4). The B-cell conformational epitope for the vaccine construct was identified using the Ellipro server (Fig. 5).

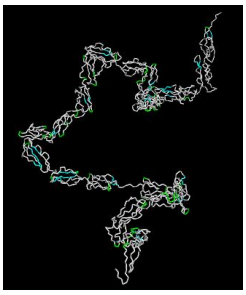

Figure 4. Tertiary structure of vaccine construct.

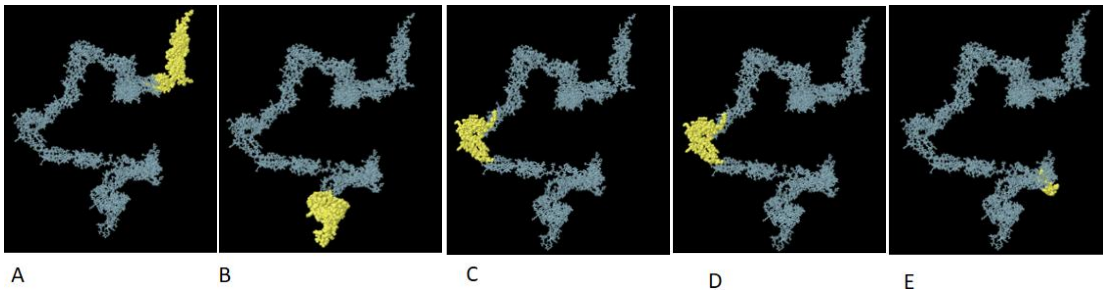

Figure 5. The 3D model of the 5 predicted conformational B-cell epitopes of the final vaccine construct. The yellow region are the conformational B-cell epitopes, while the grey areas are the residue remnant **(a)** 205 residue has a score of 0.852 **(b)** 165 residue has a score of 0.811 **(c)** 125 residue has a score of 0.742 **(d)** 24 residue has a score of 0.667 **(e)** 25 residue has a score of 0.645.

Source: Elaborated by the authors.

3.7. Refinement of the tertiary structure

Refinement of the 3D configuration entails reconstructing protein side chains, molecular dynamics simulation, and repacking to enhance the vaccine's tertiary structure. The Galaxy Refine web server was utilized for refining the vaccine's configuration, resulting in the prediction of five refined models. Model 1 was selected based on specific criteria, including a GDT-HA score of 0.8880, RMSD of 0.597, MolProbity score of 2.712, Clash score of 27.0, Poor rotamers of 0.7, and Rama favored of 75.1.

3.8. Validation of tertiary structure

Refinement provides a refined 3D vaccine model having a higher number of residues in the favored region (67.1.0%), 21.5% in the allowed area and 6.1% found in the disallowed region of Ramachandran plot (Fig. 6 and 7). Validation is often carried out to recognize errors within the structure of the final vaccine model. ProSA and PROCHECK servers provided a Z-score value of −4.07 (Fig. 8), which indicates the stability of the model. Structural validation scores obtained from ERRAT and ProSA tools proved that the overall quality of the vaccine construct meets the requirement (Oladipo *et al.*, 2022).

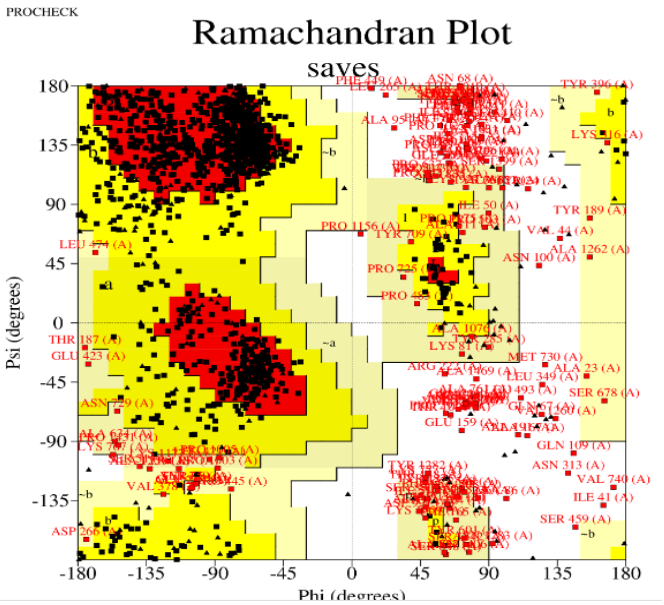

Figure 6. Ramachandran plot showing favored region of the vaccine.

Source: Elaborated by the authors.

Phi (degrees)

Plot statistics

Residues in most favored regions [A, B, L]	720	67.1%
Residues in additional allowed regions [a, b, l, p]	231	21.5%
Residues in generously allowed regions [~a, ~b, ~l, ~p]	57	5.3%
Residues in disallowed regions	65	6.1%
Number of non-glycine and non-proline residues	1073	100.0%
Number of end-residues (excl. Gly and Pro)	2	
Number of glycine residues (shown as triangles)	214	
Number of proline residues	184	
Total number of residues	1473	

Based on an analysis of 118 structures of resolution of at 2.0 Angstroms and R-factor no greater than 20%, a good quality model would be expected to have over 90% in the most favored regions.

Figure 7. Showing the favored region and number of residues.

Source: Elaborated by the authors.

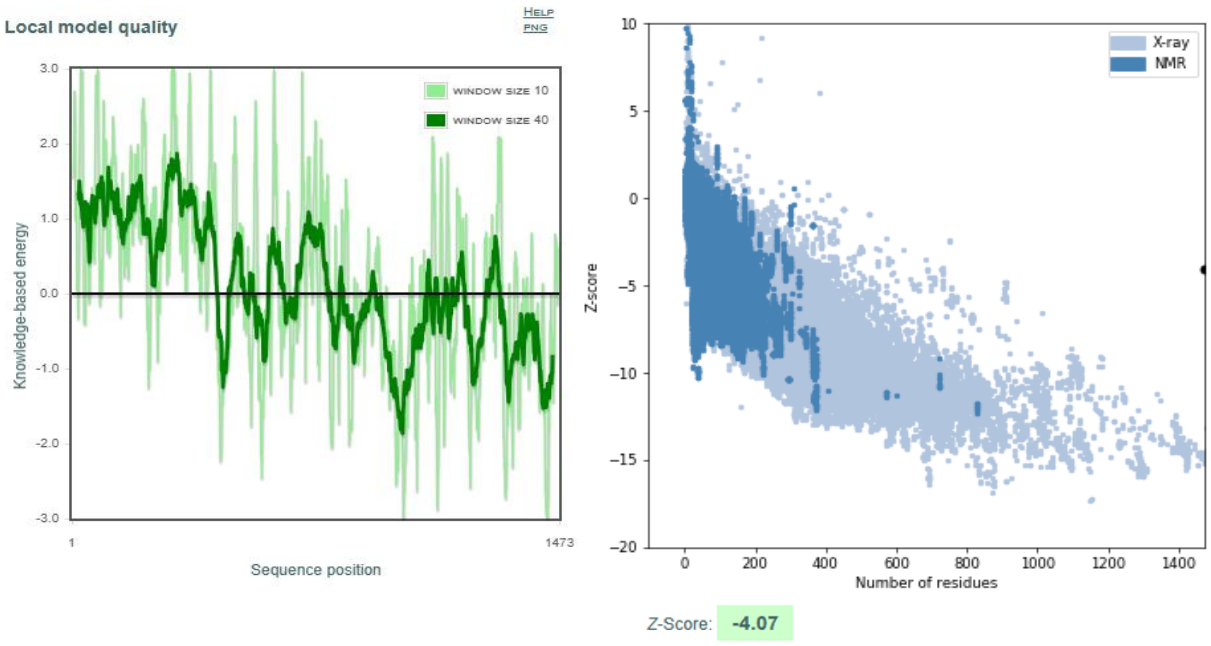

Figure 8. Graph showing model quality of the vaccine.
Source: Elaborated by the authors.

3.9. Molecular docking of the tertiary structure

The Tertiary structure was subjected to molecular docking using HDock server. The binding energy and molecular relationship of the multi-epitope subunit vaccine with TLR-2 (3a7c) and TLR-4 (4g8a) were probed by molecular docking (**Fig. 9**). One model was selected from each of the docked complexes based on their proper receptor interactions, low binding energy and center energy scores (Pandey *et al.,* 2016). The TLR 2 and TLR 4 have binding energies of -305.14 and -303.77, respectively (**Table 4**), which shows that the receptors have a high binding energy with the vaccine construct. This low binding energy score indicates strong affinities between the molecules (Oladipo *et al.,* 2023c).

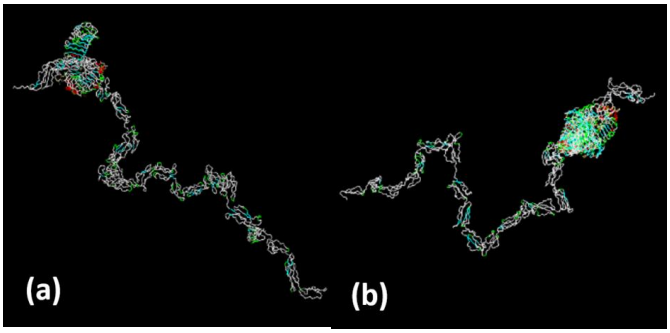

Figure 9. Molecular Docking of vaccine with TLRs **(a)** TLR-2 and vaccine construct **(b)** TLR-4 and vaccine construct.
Source: Elaborated by the authors.

Table 4. Molecular Docking against TLR-2 and TLR-4.

Dock result (rank)	TLR-4	TLR-2
Docking score	-303.77	-305.14
Confidence score	0.9559	0.9578

Source: Elaborated by the authors.

3.10. Molecular dynamic simulation

Standard Mode Analysis (NMA) was performed on the selected docked vaccine-receptor complex to investigate stability and mobility using the iMODs server. The vaccine protein and its receptor were predicted to rotate towards each other, as depicted in **Fig. 10** and **11** for TLR2 and TLR4, respectively. Hinges in regions of high deformability indicate the deformability of the vaccine-receptor complex, as shown in **Fig. 10c** and **11c** for TLR2 and TLR4, respectively. The B-factor is directly proportional to the RMS value inferred through NMA (**Fig. 10d** and **11d**). Eigenvalues for the vaccine-receptor complexes obtained from the iMODs server were 6.01e-09 and 4.75e-09 for TLR2 and TLR4, respectively (**Fig. 10e** and **11e**). Variance is inversely proportional to the Eigenvalue. Residual index graphs indicate correlated, anti-correlated, and uncorrelated pairs of residues in the variance matrix, represented by red, blue, and white colors, respectively (**Fig. 10b** and **11b**). The elastic network model generated by iMODs (**Fig. 10f** and **11f**) illustrates pairs of atoms connected by springs, with stiffer springs represented by dark grey areas. Dynamics results showed positive eigenvalues (2.27e05; 2.06e-06; 2.03e-05; 1.53e-05), which are significant for vaccine stability and rotation, consistent with previous studies (Chauhan *et al.*, 2019).

https://doi.org/10.26850/1678-4618.eq.v50.2025.e1555

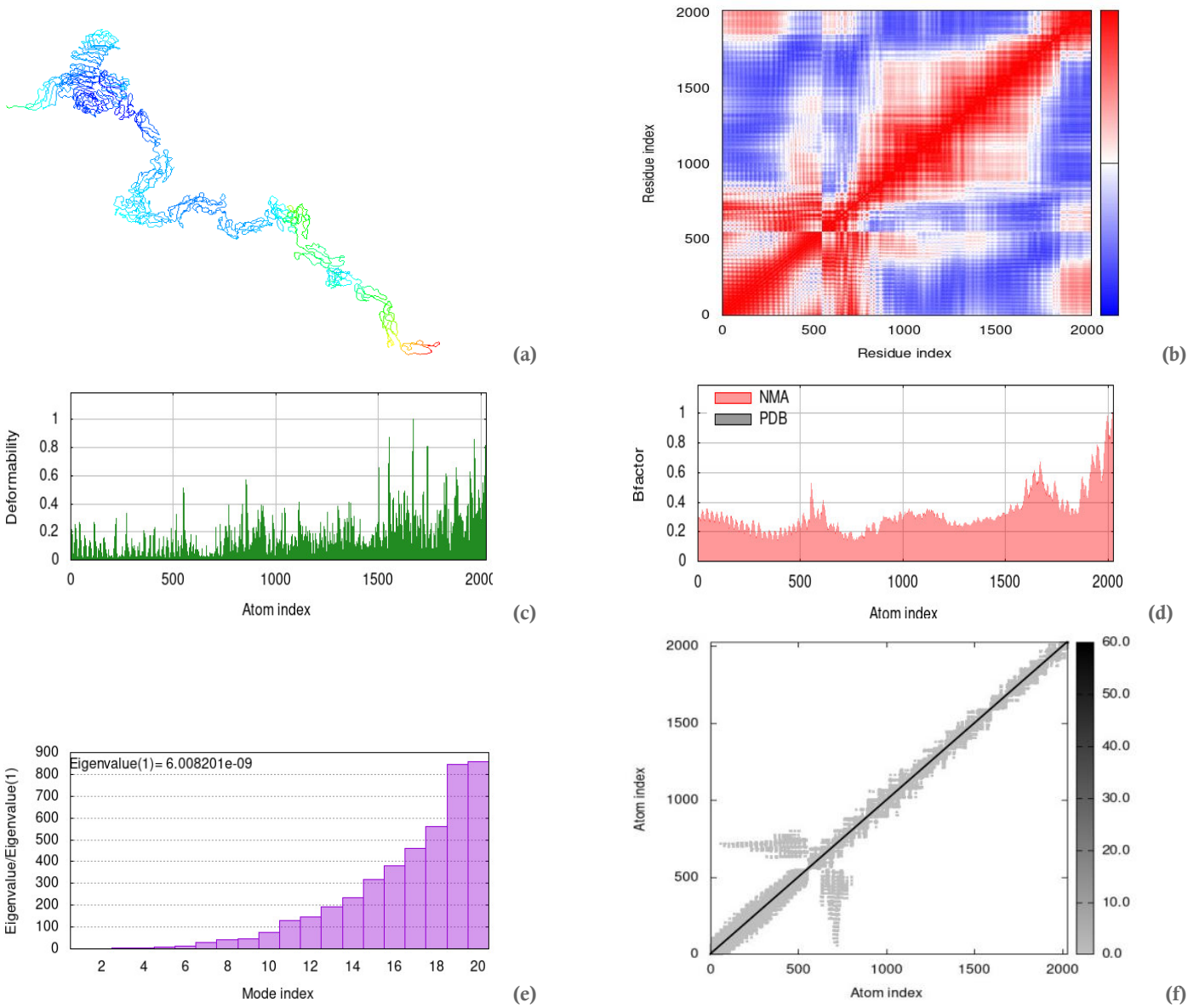

Figure 10. Molecular dynamics simulation for TLR2: **(a)** Spin prediction of the ligand-receptor interaction; **(b)** Covariance map of the ligand-receptor interaction **(c)** Deformability B-factor region of the ligand-protein interaction **(d)** Mobility B-factor of the ligand-protein interaction **(e)** Eigenvalues of the ligand-receptor interaction **(f)** Elastic network of the ligand-protein interaction.
Source: Elaborated by the authors.

https://doi.org/10.26850/1678-4618.eq.v50.2025.e1555

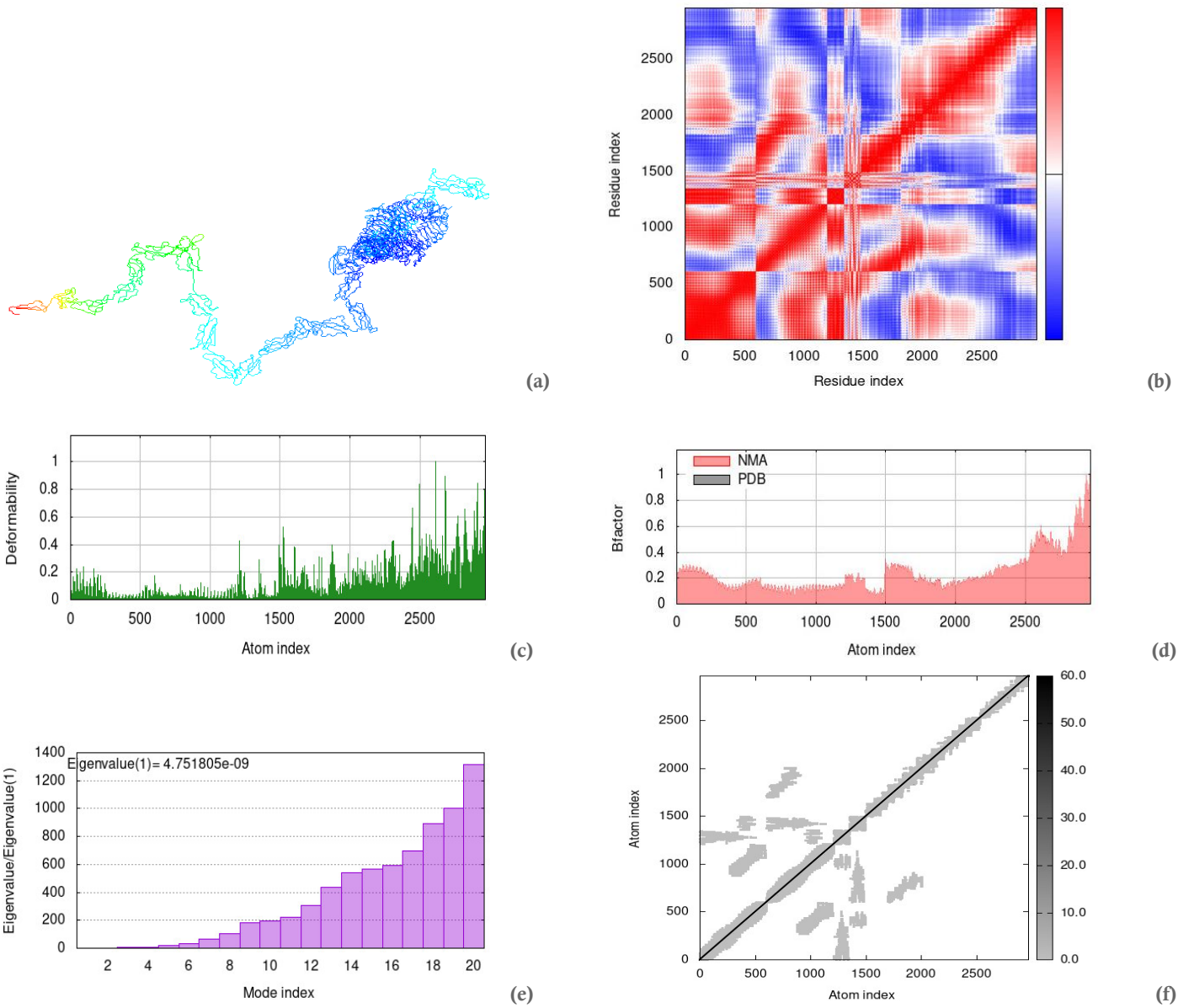

Figure 11. Molecular dynamics simulation for TLR2: **(a)** Spin prediction of the ligand-receptor interaction **(b)** Covariance map of the ligand-receptor interaction **(c)** Deformability B-factor region of the ligand-protein interaction **(d)** Mobility B-factor of the ligand-protein interaction **(e)** Eigenvalues of the ligand-receptor interaction **(f)** Elastic network of the ligand-protein interaction.
Source: Elaborated by the authors.

3.11. Codon adaptation and in silico cloning

Integrating the malaria vaccine construct into the *E. coli* expression system necessitates using JCAT and SnapGene servers. Adapting the vaccine to the *E. coli* K12 strain predicted a GC content of 59.31%, a Codon Adaptation Index (CAI) of 0.91. It translated the protein sequence back to nucleotides compatible with *E. coli* codons. The back-translated nucleotide sequence was incorporated into the *E. coli* expression system using the restriction enzymes ECORI (192) and BAMHI (4106) as cloning sites (**Fig. 12**). The solubility of the overexpressed recombinant protein in the *E. coli* host is crucial for biochemical and functional investigations. Therefore, adapting the vaccine model into an *E. coli* expression system is an essential step in vaccine design, and codon adaptation is a preferred method for achieving efficient expression of foreign genes in a host. This is because when the codons used by the host differ from those of the organism's genes, lower expression rates may occur if the genes are not adapted. Hence, we adapted the final vaccine protein sequences to the *E. coli* strain K12 using the JCAT server and obtained satisfactory results. JCAT also back translated the protein sequences to nucleotides, which were then cloned into the *E. coli* pET28a (+) vector using the ECORI (192) and BAMHI (4106) restriction sites, resulting in a total clone length of 9.2 Kbp. The target sequence was encoded between 6-histidine residues, which would facilitate purification purposes.

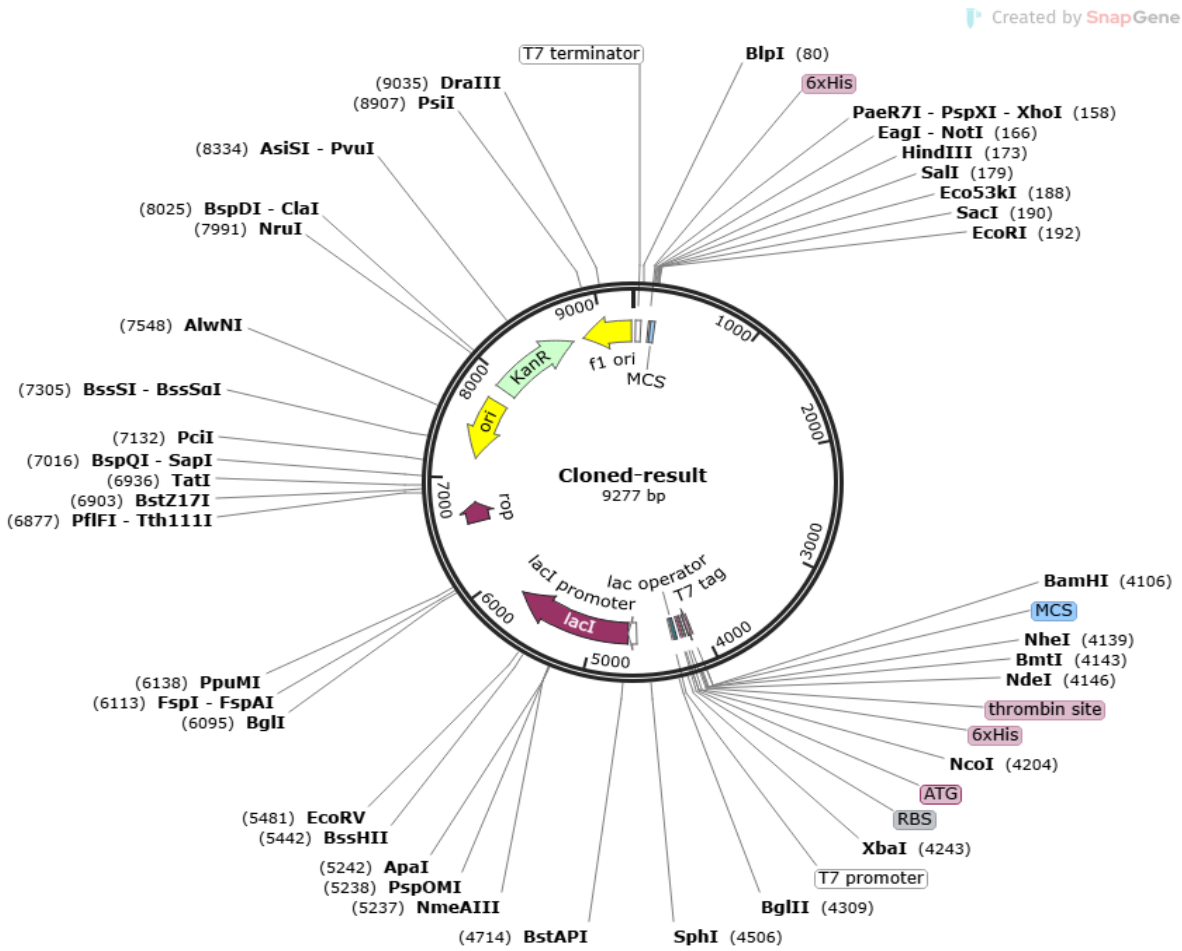

Figure 12. In silico cloning for adapted vaccine into pET28a (+) vector.
Source: Elaborated by the authors.

4. Conclusions

Tropical regions characterized by high temperatures and humidity, particularly in South Asia and Africa, are highly susceptible to malaria. Achieving malaria eradication requires the implementation of innovative control techniques. This study utilized protein sequences eliciting various T-cell (HTL and CTL) and B-cell epitopes in an immunoinformatics approach to develop a potential vaccine. The results of this investigation demonstrate that the final construct has successfully fulfilled the designed criteria for malaria vaccine development. However, this computational work necessitates experimental validation. In vitro and in vivo tests are essential to assess the immunogenicity and safety of the potential vaccine.

Authors' contribution

Conceptualization: Elijah Kolawole Oladipo; **Data curation:** James Akinwumi Ogunniran; **Formal Analysis:** Samuel Nzube Nwosu; **Funding acquisition:** Not applicable; **Investigation:** James Akinwumi Ogunniran; **Methodology:** James Akinwumi Ogunniran; **Project administration:** Not applicable; **Resources:** Not applicable; **Software:** Kehinde Oluyemi Ajayi; Oluseyi Rotimi Taiwo; **Supervision:** Elijah Kolawole Oladipo; **Validation:** Olaoluwa Kehinde Alao; Adeola Christianah Ogunwole; **Visualization:** Kemiki Olalekan Ademola; Michael Asebake Ockiya; **Writing – original draft:** James Akinwumi Ogunniran; Caleb Enejoh Omede; **Writing – review & editing:** James Akinwumi Ogunniran; Anthony Godswill Imolele.

Data availability statement

All datasets analyzed in this research are all publicly available at the National Centre of Biotechnology Information (NCBI) and the Universal Protein Resource (UNIPROT) Server. It could be made available upon request.

Funding

Not applicable.

Acknowledgments

We appreciate Helix Biogen Institute, Ogbomoso, Oyo State, Nigeria for their technical support during this research work.

Conflict of interest

The authors declare that there is no conflict of interest.

References

Amir, A.; Parisa, V.; Somayeh, J.; Gholamreza, A. S. A multi-epitope vaccine designed against blood-stage of malaria: an immunoinformatic and structural approach. *Sci. Rep.* **2022**, *12*, 11683. https://doi.org/10.1038/s41598-022-15956-3

Amlabu, E.; Mensah-Brown, H.; Nyarko, P. B.; Akuh, O. A.; Opoku, G.; Ilani, P.; Oyagbenro, R.; Asiedu, K.; Aniweh, Y.; Awandare, G. A.

Functional Characterization of Plasmodium falciparum Surface-Related Antigen as a Potential Blood-Stage Vaccine Target. *J Infect Dis*. **2018**, *218* (5), 778-790. https://doi.org/10.1093/infdis/jiy222

Biamonte, M. A.; Wanner, J.; Le Roch, K. G. Recent advances in malaria drug discovery. *Bioorg. Med. Chem*. **2013**, *23* (10), 2829–2843. https://doi.org/10.1016/j.bmcl.2013.03.067

Chauhan,V.; Rungta, T.; Goyal, K.; Singh, M. P. Designing a multi-epitope based vaccine to combat Kaposi Sarcoma utilizing immunoinformatics approach. *Sci. Rep*. **2019**, *9* (1), 2517. https://doi.org/10.1038/s41598-019-39299-8

Chauhan, V.; Singh, M. P. Immuno-informatics approach to design a multi-epitope vaccine to combat cytomegalovirus infection. *Eur J Pharmaceut Sci*. **2020**, *147*, 105279. https://doi.org/10.1016/j.ejps.2020.105279

Chaves, T. D. S. S.; Monteiro, W. M.; Alves, J. R.; Lacerda, M.; Lopes, M. H. Pre-travel malaria chemoprophylaxis counselling in a public travel medicine clinic in São Paulo. Brazil. *Malar. J*. **2017**, *16*, 64. https://doi.org/10.1186/s12936-017-1713-3

Crompton, P. D.; Pierce, S. K.; Miller, L. H. Advances and challenges in malaria vaccine development. *J. Clin. Invest*. **2010**, *120* (12), 4168–4178. https://doi.org/10.1172/JCI44423

Dimitrov, I.; Bangov, I.; Flower, D. R.; Doytchinova, I. AllerTOP v. 2—a server for in silico prediction of allergens. *J Mol Model*. **2014**, *20* (6), 2278. https://doi.org/10.1007/s00894-014-2278-5

Doytchinova, I. A.; Flower, D. R. VaxiJen. A server for prediction of protective antigens, tumour antigens and subunit vaccines. *BMC Bioinf*. **2007**, *8*, 4. https://doi.org/10.1186/1471-2105-8-4

Garg, V. K.; Avashthi, H.; Tiwari, A.; Jain, P.A.; Ramkete, P. W.; Kayastha, A. M.; Singh, V. K. MFPPI–Multi FASTA ProtParam interface. *Bioinformation*. **2016**, *12* (2), 74. https://doi.org/10.6026/97320630012074

Grote, A.; Hiller, K.; Scheer, M.; Münch, R.; Nörtemann, B.; Hempel, D. C.; Jahn, D. JCat. a novel tool to adapt codon usage of a target gene to its potential expression host. *Nucleic Acids Res*. **2005**, *33* (2), W526–W531. https://doi.org/10.1093/nar/gki376

Heo, L.; Park, H.; Seok, C. GalaxyRefine: Protein structure refinement driven by side-chain repacking. *Nucleic Acids Res*. **2013**, *41*, W384–W388. https://doi.org/10.1093/nar/gkt458

Holder, A. A. The carboxy-terminus of merozoite surface protein 1: structure, specific antibodies and immunity to malaria. *Parasitology*. **2009**, *136* (12), 1445–1456. https://doi.org/10.1017/S0031182009990515

Ito, M.; Hayashi, K.; Minamisawa, T.; Homma, S.; Koido, S.; Shiba, K. Encryption of agonistic motifs for TLR4 into artificial antigens augmented the maturation of antigenpresenting cells. *PLoS One*. **2017**, *12* (11), e0188934. https://doi.org/10.1371/journal.pone.0188934

Kadekoppala, M.; O'Donnell, R. A.; Grainger, M.; Crabb, B. S.; Holder, A. A. Deletion of the *Plasmodium falciparum* merozoite surface protein 7 gene impairs parasite invasion of erythrocytes. *Eukaryot Cell*. **2008**, *7* (12), 2123–2132. https://doi.org/10.1128/ec.00274-08

Kalita, P.; Lyngdoh, D. L.; Padhi, A. K.; Shukla, H.; Tripathi, T. Development of multi-epitope driven subunit vaccine against Fasciolagigantica using immunoinformatics approach. *Int. J. Biol. Macromol*. **2019**, *138*, 224–233. https://doi.org/10.1016/j.ijbiomac.2019.07.024

Kristian, E. S.; Scott, E. L.; Lirong, S.; Melanie, J. S.; Anke, H.; Christine, S. H.; Ashley, M. V.; Timothy, A.S.; Robert, L. M.; Stefan, H. I. K. Interrogating the *Plasmodium* Sporozoite Surface: Identification of Surface-Exposed Proteins and Demonstration of Glycosylation on CSP and TRAP by Mass Spectrometry-Based Proteomics. *PLOS Pathog*. **2016**, *12* (4), e1005606. https://doi.org/10.1371/journal.ppat.1005606

Laskowski, R. A.; MacArthur, M. W.; Thornton, J. M. https://onlinelibrary.wiley.com/ (PROCHECK: Validation of protein-structure coordinates). Chapter 25.2, 2006. https://doi.org/10.1107/97809553602060000724

Laurens, M. B. RTS, S/AS01 vaccine (Mosquirix™): an overview. *Hum Vaccin Immunother*. **2020**, *16* (3), 480–489. https://doi.org/10.1080/21645515.2019.1669415

Lee, H. W.; Kim, M. J.; Park, M. Y.; Han, K. H.; Kim, J. The conserved proline residue in the LOB domain of LBD18 is critical for DNA-binding and biological function. *Mol Plant*. **2013**, *6* (5), 1722–1725. https://doi.org/10.1093/mp/sst037

Li, M.; Li, M.; Lin, H.; Wang, J.; Jin, Y.; Han, F. Characterization of the novel T4-like Salmonella enterica bacteriophage STP4-a and its endolysin. *Arch Virol*. **2016**, *161* (2), 377–384. https://doi.org/10.1007/s00705-015-2647-0

Lindner, S. E.; Miller, J. L.; Kappe, S. H. Malaria parasite pre-erythrocytic infection: preparation meets opportunity. *Cell. Microbiol*. **2012**, *14* (3), 316–324. https://doi.org/10.1111/j.1462-5822.2011.01734.x

López-Blanco, J. R.; Aliaga, J. I.; Quintana-Ortí, E. S.; Chacón, P. iMODS. Internal coordinates normal mode analysis server. *Nucleic Acids Res*. **2014**, *42* (W1), W271–W276. https://doi.org/10.1093/nar/gku339

Magnan, C. N.; Zeller, M.; Kayala, M. A.; Adam, V.; Randall, A.; Felgner, P. L.; Baldi Pierre. High-throughput prediction of protein antigenicity using protein microarray data. *Bioinformatics*. **2010**, *26* (23), 2936–2943. https://doi.org/10.1093/bioinformatics/btq551

Maier, A. G.; Cooke, B. M.; Cowman, A. F.; Tilley, L. Malaria parasite proteins that remodel the host erythrocyte. *Nature Reviews. Microbiology*. **2009**, *7* (5), 341–354. https://doi.org/10.1038/nrmicro2110

Oladipo EK, Adeniyi MO, Ogunlowo MT, Irewolede BA, Adekanola VO, Oluseyi GS, Omilola JA, Udoh AF, Olufemi SE, Adediran DA, Olonade A, Idowu UA, Kolawole OM, Oloke JK, Onyeaka H. Bioinformatics Designing and Molecular Modelling of a Universal mRNA Vaccine for SARS-CoV-2 Infection. *Vaccines (Basel)*. **2022**, *10* (12), 2107. https://doi.org/10.3390/vaccines10122107

Oladipo, E. K.; Ajayi, A. F.; Ariyo, O. E.; Onile, S. O.; Jimah, E. M.; Ezediuno, L. O.; Adebayo, O. I.; Adebayo, E. T.; Odeyemi, A. N.; Oyeleke, M. O.; Oyewole, M. P.; Oguntomi, A. S.; Akindiya, O. E.; Olamoyegun, B. O.; Aremu, V.; Arowosaye, A. O.; Aboderin, D. O.; Bello, H. B.; Senbadejo, T. Y.; Awoyelu, E. H.; Oladipo, A. A.; Oladipo, B. B.; Ajayi, L. O.; Majolagbe, O. N.; Oyawoye, O. M.; Oloke, J. K. Exploration of surface glycoprotein to design multi-epitope vaccine for the prevention of Covid-19. *Inform. Med. Unlocked*. **2020**, *21*, 100438. https://doi.org/10.1016/j.imu.2020.100438

Oladipo, E. K.; Jimah, E. M.; Irewolede, B. A.; Folakanmi, E. O.; Olubodun, O. A.; Adediran, D. A.; Akintibubo, S. A.; Odunlami, F. D.; Olufemi, S. E.; Ojo, T. O.; Akinro, O. P.; Hezekiah, O. S.; Olayinka, A. T.; Abiala, G. A.; Idowu, A. F.; Ogunniran, J. A.; Ikuomola, M. O.; Adegoke, H. M.; Idowu, U. A.; Akindiya, O. E.; Adelusi T. I. Bioinformatics analysis of structural protein to approach a vaccine candidate against Vibrio cholerae infection. *Immunogenetics*. **2023a**, *75* (2). 99–114. https://doi.org/10.1007/s00251-022-01282-5

Oladipo, E. K.; Jimah, E. M.; Irewolede, B. A.; Folakanmi, E. O.; Olubodun, O. A.; Adediran, D. A.; Akintibubo, S. A.; Odunlami, F. D.; Olufemi, S. E.; Ojo, T. O.; Akinro, O. P.; Hezekiah, O. S.; Olayinka, A. T.; Abiala, G. A.; Idowu, A. F.; Ogunniran, J. A.; Ikuomola, M. O.; Adegoke, H. M.; Idowu, U. A.; Akindiya, O. E.; Oluwasanya, G. J.; Akanbi, G. M.; Bamigboye, F. O.; Aremu, R. O.; Awobiyi, H. O.; Kolapo, K. T.; Oluwasegun, J. A.; Olatunde, S. K.; Adelusi, T. I. Immunoinformatics design of multi-epitope peptide for the diagnosis of *Schistosoma haematobium* infection. *J Biomol Struct Dyn*. **2023b**, *41* (14), 6676–6683. https://doi.org/10.1080/07391102.2022.2111358

Oladipo, E. K.; Ojo, T. O.; Olufemi, S. E.; Irewolede, B. A.; Adediran, D. A.; Abiala, A. G.; Hezekiah, O. S.; Idowu, A. F.; Oladeji, Y. G.; Ikuomola, M. O.; Olayinka, A. T.; Akanbi, G. O.; Idowu, U. A.; Olubodun, O. A.; Odunlami, F. D.; Ogunniran, J. A.; Akinro, O. P.; Adegoke, H. M.; Folakanmi, E. O.; Usman, T. A, Oladokun, E. F.; Oluwasanya, G. J.; Awobiyi, H. O.; Oluwasegun, J. A.; Akintibubo, S. A.; Jimah, E. M. Proteome based analysis of circulating SARS-CoV-2 variants: approach to a universal vaccine candidate. *Genes Genomics*. **2023c**, *45* (12), 1489–1508. https://doi.org/10.1007/s13258-023-01426-1

Oladipo, E. K.; Adeyemo, S. F.; Akinboade, M. W.; Akinleye, T. M.; Siyanbola, K. F.; Adeogun, P. A.; Ogunfidodo, V. M.; Adekunle, C. A.; Elutade, O. A.; Omoathebu, E. E.; Taiwo, B.O.; Akindiya, E. O.; Ochola, L.; Onyeaka, H. Utilizing Immunoinformatics for mRNA Vaccine Design against Influenza D Virus. *BioMedInformatics*. **2024a**, *4*, 1572–1588. https://doi.org/10.3390/biomedinformatics4020086

Oladipo, E. K.; Ojo, T. O.; Elegbeleye, O. E.; Bolaji, O. Q.; Oyewole, M. P.; Ogunlana, A. T.; Olalekan, E. O.; Abiodun, B.; Adediran, D. A.; Obideyi, O. A.; Olufemi, S. E.; Salamatullah, A. M.; Bourhia, M.; Younous, Y. A.; Adelusi, T. I. Exploring the nuclear proteins, viral capsid protein, and early antigen protein using immunoinformatic and molecular modeling approaches to design a vaccine candidate against Epstein Barr virus. *Sci. Rep.* **2024b**, *14* (1), 16798. https://doi.org/10.1038/s41598-024-66828-x

Oluwagbemi, O. O.; Oladipo, E. K.; Kolawole, O. M.; Oloke, J. K.; Adelusi, T. I.; Irewolede, B. A.; Dairo, E. O.; Ayeni, A. E.; Kolapo, K. T.; Akindiya, O. E.; Oluwasegun, J. A.; Oluwadara, B. F.; Fatumo, S. Bioinformatics, Computational Informatics, and Modeling Approaches to the Design of mRNA COVID-19 Candidates. *Computation.* **2022**, *10* (7), 117. https://doi.org/10.3390/computation10070117

Pandey, K.; Sharma, M.; Saarav, I.; Singh, S.; Dutta, P.; Bhardwaj, A.; Sharma, S. Analysis of the DosRregulon genes to select cytotoxic T lymphocyte epitope, specific vaccine candidates, using a reverse vaccinology approach. *Int. J. Mycobacteriol*. **2016**, *5* (1), 34–43. https://doi.org/10.1016/j.ijmyco.2015.10.005

Pandey, R. K.; Bhatt, T. K.; Prajapati, V. K. Novel immunoinformatics approaches to design multi-epitope subunit vaccine for malaria by investigating Anopheles salivary protein. *Sci Rep*. **2018**, *8* (1), 1125. https://doi.org/10.1038/s41598-018-19456-1

Pandey, R. K.; Ojha, R.; Aathmanathan, V. S.; Krishnan, M.; Prajapati, V. K. Immunoinformatics approaches to design a novel multi-epitope subunit vaccine against HIV infection. *Vaccine*. **2018**, *36* (17), 2262–2272. https://doi.org/10.1016/j.vaccine.2018.03.042

Ponomarenko, J.; Bui, H. H.; Li, W.; Fusseder, N.; Bourne, P. E.; Sette, A.; Peters, B. ElliPro: a new structure-based tool for the prediction of antibody epitopes. *BMC Bioinf.* **2008**, *9* (1), 514. https://doi.org/10.1186/1471-2105-9-514

Saha, S.; Raghava, G. P. S. Prediction of Continuous B-cell Epitopes in an Antigen Using Recurrent Neural Network. *Proteins*. **2006**, *65* (1), 40–48. https://doi.org/10.1002/prot.21078

Schumacher, R. F.; Spinelli, E. Malaria in Children. *J. Hematol. Infect. Dis*. **2012**, *4*, e2012073. https://doi.org/10.4084/MJHID.2012.073

Sharma, N.; Naorem, L. D.; Jain, S.; Raghava, G. P. S. ToxinPred2: An improved method for predicting toxicity of proteins. *Briefings Bioinform.* **2022**, *23*, bbac174. https://doi.org/10.1093/bib/bbac174

Singh, B.; Kim Sung, L.; Matusop, A.; Radhakrishnan, A.; Shamsul, S. S.; Cox-Singh, J.; Thomas, A.; Conway, D. J. A large focus of naturally acquired Plasmodium knowlesi infections in human beings. *Lancet*. **2004**, *363* (9414), 1017–1024. https://doi.org/10.1016/S0140-6736(04)15836-4

Sinnis, P.; Zavala, F. The skin stage of malaria infection: biology and relevance to the malaria vaccine effort. *Future Microbiol*. **2008**, *3*, 275–278. https://doi.org/10.2217/17460913.3.3.275

Srinivasan, P.; Beatty, W. L.; Diouf, A.; Herrera, R.; Ambroggio, X.; Moch, J. K.; Tyler, J. S.; Narum, D. L.; Pierce, S. K.; Boothroyd, J. C.; Haynes, J. D.; Miller, L. H. Binding of Plasmodium merozoite proteins RON2 and AMA1 triggers commitment to invasion. *Proc Natl Acad Sci*. **2011**, *108* (32), 13275–13280. https://doi.org/10.1073/pnas.1110303108

Tahmoorespur, M.; Nazifi, N.; Pirkhezranian, Z. In silico prediction of B-cell and T-cell epitopes of protective antigen of Bacillus anthracis in development of vaccines against anthrax. *Iran J. Appl. Anim Sci*. **2017**, *7* (3), 429–436.

World Health Organization (WHO). *World Malar. Rep.* 2022, 1–186; http://www.who.int/malaria/publications/world-malaria-report-2022/report/en/

Yan, Y.; Tao, H.; He, J.; Huang, S.Y. The HDOCK server for integrated protein-protein docking. *Nat. Protoc.* **2020**, *15* (5), 1829–1852. https://doi.org/10.1038/s41596-020-0312-x

Zhang, W.; Liu, J.; Niu, Y.Q.; Wang, L.; Hu, X. A Bayesian regression approach to the prediction of HC-II binding affinity. *Comput. Methods. Progr. Biomed*. **2008**, *92* (1), 1–7. https://doi.org/10.1016/j.cmpb.2008.05.002

Zhao, J. W.; Yan, M.; Shi, G.; Zhang, S. L.; Ming, L. In silico identification of cytotoxic T lymphocyte epitopes encoded by RD5 region of Mycobacterium tuberculosis. *J. Inf. Dev. Countries*. **2017**, *11* (10), 806–810. https://doi.org/10.3855/jidc.7207

Zhou, X.; Zheng, W.; Li, Y.; Pearce, R.; Zhang, C.; Bell, E. W.; Zhang, G.; Zhang, Y I-TASSER-MTD: a deep-learning-based platform for multi-domain protein structure and function prediction. *Nature Protocols*. **2022**, *17*, 2326–2353.